05FFL-188

Development and Validation of an Impedance Transfer Model for High Speed Engines

Sam Zimmerman, Dan Cordon, Michael Anderson, and Steven Beyerlein
Mechanical Engineering, University of Idaho

Copyright © 2005 SAE International

ABSTRACT

Acoustical tuning of intake manifolds is a common practice used to achieve gains in volumetric efficiency in a pre-determined region on the torque curve. Many methods exist for acoustical tuning of the intake including a variation of the Helmholtz resonator model by Engelman as well as the organ pipe models by Ricardo and Platner. In this work a new intake tuning model has been developed using an Impedance Transform Model along with a minimal set of limiting assumptions. Unlike the models of Engelman and Platner, this model can accommodate any intake geometry. The model can also be used to analyze specific points in the intake system or the entire system rather than just the intake runners. Model verification consisted of resonance testing of three different Helmholtz resonators as well as dynamometer testing of a Honda CBR F3 four-stroke SI engine using three different intake system geometries. The different intake systems and Helmholtz resonators were designed such that each would produce different resonant frequencies for proper model verification. The model accurately predicted the resonate frequencies of each different Helmholtz resonator and the torque peak produced by each intake system iteration.

INTRODUCTION

Acoustic modeling of unsteady air flow into internal combustion engines provides an opportunity to maximize torque output at a pre-determined operating speed or to increase torque over a pre-determined speed range. By designing a system to resonate at specific frequencies, a greater charge of air can be packed into the combustion chamber, increasing the volumetric efficiency of the engine, resulting in these performance gains. Many methods have historically been used to determine the correct runner length and cross-sectional area for intake manifolds in internal combustion engines. The runner length is defined as the length of the flow channel which extends from the intake port on the head to the point at which the individual runners branch out from a manifold, airbox, or plenum. Three historical models by Ricardo, Platner, and Engelman provide the starting point for this research. Each of the models mentioned above focuses on the runner length upstream of the intake port on the head rather than the entire intake system and identifies a single resonance which is assumed to correspond to an optimal volumetric efficiency. None of the above models can identify anti-resonances in the intake system which would diminish acoustic effects and thereby decrease volumetric efficiency. Likewise, the models of Ricardo, Platner, and Engelman fail to incorporate any part of the intake system upstream of the runners into the model. Three questions underlie the current research effort:

- What is the impact of a specific intake tuning across the entire speed spectrum?
- How much is each resonance and anti-resonance impacted by changes in different components of the intake system?
- How is engine power output influenced by the location of resonances and anti-resonances across the speed range?

An analytic method was used to answer the first two questions whereas an empirical method was used to answer the third question. All three questions involve the volumetric efficiency which is defined in equation (1).

$$\eta_v = \frac{m_{mix}}{\rho_{air} \cdot V_{cyl}} \qquad (1)$$

where

η_v = volumetric efficiency

m_{mix} = mass of the fuel/air mixture in the combustion chamber

ρ_{air} = density of the atmospheric air

V_{cyl} = displaced volume of a cylinder

A model for understanding how volumetric efficiency impacts engine torque is given by equation (2).

$$\tau = \frac{\eta_m \cdot \eta_i \cdot \eta_c \cdot (-\Delta H) \cdot \frac{F}{A} \cdot \eta_v \cdot \rho_{air} \cdot V}{2 \cdot \pi \cdot n_R} \qquad (2)$$

where

τ = torque
η_m = mechanical efficiency
η_i = indicated thermal efficiency
η_c = combustion efficiency
ΔH = heating value of fuel
$\frac{F}{A}$ = fuel to air ratio (mass)
ρ_{air} = density of ambient air
V = engine displacement
n_R = number of cycles per intake stroke

Combustion efficiency will change with engine load, although it is virtually unchanged by engine speed. In addition, combustion efficiency varies between approximately 90% - 95% as load changes, having little effect on engine torque. Indicated thermal efficiency is also independent of engine speed. Likewise, the heating value, fuel to air ratio, density, engine displacement, and number of cycles per intake stroke are all independent of engine speed. Because of this, variances in torque as engine speed changes is overwhelmingly controlled by acoustical changes in the intake and exhaust systems which causes the volumetric efficiency to change as engine speed changes.

Typical volumetric and mechanical efficiency curves are shown in Figure 1. Fluid dynamics through the intake system will vary somewhat with engine speed and will cause some changes in volumetric efficiency. Acoustic resonance, on the other hand, can have a profound impact on volumetric efficiency and this is a strong function of engine speed. Resonance effects can influence both the intake and the exhaust by having compression waves that hit the intake valve and exhaust valve at the correct time in the cycle.

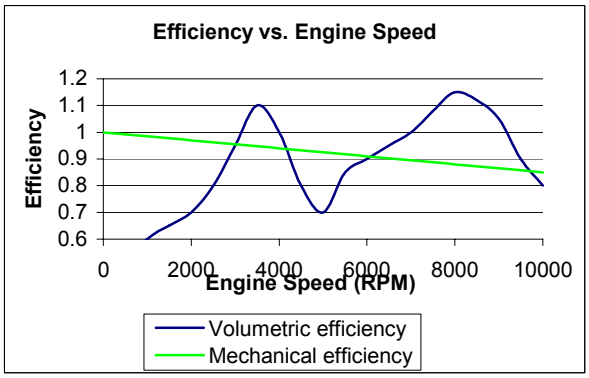


Figure 1. Typical mechanical and volumetric efficiency curves for an I.C. engine.

MODEL VERIFICATION

HISTORICAL MODELS

Previous methods of acoustical tuning include the organ pipe analogy, used by Ricardo and Platner, and the Helmholtz resonator analogy pioneered by Engelman and further refined in Eberhard and Thompson [1-5]. Other methods described at the end of the section we studied but are not compared in detail in this paper due to brevity.

It can be observed by Ricardo's equation of

$$\frac{5.4 \cdot 10^7}{3N^{1.85}} \le L \le \frac{5.4 \cdot 10^7}{N^{1.85}} \qquad (3)$$

where

N = Engine speed in RPM
L = Runner Length (ft.)

that the analysis was empirical rather than analytical [1]. Equation (3) does not take any intake or cylinder geometry into account explicitly, but by inspection the equation appears to have been based solely on empirical data. This would mean that it implicitly took into account the geometry of the entire system and could only be used on Ricardo's specific engine. In addition, the calculated intake runner length can vary by a factor of three in this analysis.

Platner's equation of

$$L = \frac{6c}{N} \qquad (4)$$

with L and N was representing the same values as in equation (3) and c being the speed of sound in feet per second, was derived from the same acoustical wave theory which describes organ pipes [2]. When analyzing an organ pipe acoustically, one assumption that is generally made is that there is zero load impedance at

the end of the pipe, or the pipe opens to atmosphere. This is clearly not the case in the engine where there are intake valves and a cylinder downstream of the organ pipe. Equation (4) does take into account the largest contributor to the acoustic supercharging effect, the runner, and will output a length corresponding to the peak torque at a given engine speed. It will not take into account the any other intake or cylinder geometries nor will it offer any information on the effects to the torque curve at different engine speeds.

Engelman, Eberhard, and Thompson were the first published authors to attempt to incorporate an analytical formula for acoustical tuning of intake manifolds that would introduce the cylinder into the analysis, thus incorporating the theory of Helmholtz resonators into the intake analysis. By analyzing the runner and cylinder combined, they were able to predict the engine speed at which the maximum volumetric efficiency will occur, via equation (5) [3-5].

$$N = \frac{162}{k} \cdot c \sqrt{\frac{A}{L \cdot V}} \sqrt{\frac{R-1}{R+1}} \qquad (5)$$

where

N = engine speed (RPM)
k = ratio of Helmholtz frequency to engine frequency (2.0-2.5 range)
c = speed of sound (ft/s)
A = pipe cross sectional area (in^2)

Although equation (5) does take the cylinder geometry into account, it does not analyze the effects of any part of the intake system upstream of the runners. In addition, equation (5) resembles equations (3) and (4) in that it helps to set the intake geometry for only the peak torque and will not work to analyze what effects this intake setup will have over the whole range of engine speeds.

Other historical models include Heywood in which he discusses a finite element method for analyzing unsteady flow in intake and exhaust systems and Blair, who looks at the issue from more of an acoustical based model [6, 7]. Blair's model uses the same theory presented in the following section in an analogous form. Winterbone and Pearson provide a comprehensive approach to the subject, providing multiple methods for determining unsteady flow in pipes; capitalizing on the works of Blair, Engelman, and others [8].

IMPEDANCE TRANSFORM MODEL

Wave propagation in an intake system is governed by conservation of momentum, conservation of mass, and the equation of state as shown in equations (6), (7), and (8) respectively.

$$\rho \cdot \frac{\partial \vec{u}}{\partial t} + \rho \cdot \vec{u} \cdot \nabla \vec{u} = -\nabla P + \frac{4}{3} \cdot \eta \cdot \nabla \cdot (\nabla \cdot \vec{u}) - \eta \cdot \nabla \times \nabla \times \vec{u} \qquad (6)$$

$$\frac{\partial \rho}{\partial t} + \nabla \cdot (\rho \cdot \vec{u}) = 0 \qquad (7)$$

$$\frac{P}{P_o} = \left(\frac{\rho}{\rho_o} \right)^{\chi} \qquad (8)$$

where

ρ = total density
$\vec{u}$ = particle velocity
P = total pressure
η = shear viscosity
P_o = Atmospheric pressure
χ = coefficient of isentropic compression

First we must make the following assumptions:

- Acoustic compressions are small
- Particle movements associated with acoustic compressions are small
- No viscous forces
- Ambient quantities are not spatially dependant
- Adiabatic compression.

These assumptions allow the conservation of momentum equation to become

$$\frac{\partial \rho'}{\partial t} + \rho_o \nabla \cdot \vec{u} = 0 \qquad (9)$$

and the conservation of mass equation becomes

$$\rho_o \frac{\partial \vec{u}}{\partial t} = -\nabla p \qquad (10)$$

where

ρ' = acoustic density
ρ_o = ambient density
p = acoustic pressure.

The equation of state equation can be approximated via a Taylor's series as shown in equation (11).

$$P - P_o = \left.\frac{\partial P}{\partial \rho}\right|_{\rho=\rho_o} \rho' + \frac{1}{2}\left.\frac{\partial^2 P}{\partial \rho^2}\right|_{\rho=\rho_o} (\rho')^2 + ... + H.O.T. \quad (11)$$

Recognizing that $p = P - P_o$ and neglecting higher order terms, the equation of state is further simplified to

$$p = \left.\frac{\partial P}{\partial \rho}\right|_{\rho=\rho_o} \rho' \quad (12).$$

The isentropic bulk modulus, β, is defined in equation (13).

$$\beta \equiv \rho_o \left.\frac{\partial P}{\partial \rho}\right|_{\rho=\rho_o} \quad (13)$$

Substituting equation (13) into equation (12) yields equation (14).

$$p = \frac{\beta}{\rho_o} \rho' \quad (14)$$

Next, equation (14) is substituted into the conservation of momentum equation (9) to eliminate ρ'. The derivative with respect to time is then taken to produce equation (15).

$$\frac{\rho_o}{\beta}\frac{\partial^2 p}{\partial t^2} + \rho_o \frac{\partial}{\partial t}(\nabla \cdot \vec{u}) = 0 \quad (15)$$

Equation (14) is then substituted into the conservation of mass equation (10) and both sides are dotted with ∇. The result is shown as equation (16).

$$\rho_o \frac{\partial}{\partial t}(\nabla \cdot \vec{u}) = -\nabla^2 p \quad (16)$$

Combining equations (15) and (16) and recognizing that $c = \sqrt{\frac{\beta}{\rho_o}}$ where c is the speed of sound in the medium yields the fundamental wave equation as shown in equation (17).

$$\nabla^2 p - \frac{1}{c}\frac{\partial^2 p}{\partial t^2} = 0 \quad (17)$$

For the purpose of analyzing intake systems, equation (17) will be regarded as a one-dimensional equation with the "x" variable representing the position within the intake system, with x = 0 being the point closest to the piston or closed intake valve. Thus, equation (17) becomes

$$\frac{\partial^2 p}{\partial x^2} - \frac{1}{c}\frac{\partial^2 p}{\partial t^2} = 0 \quad (18).$$

The general solution for the second order, partial differential equation above (D'Albert's solution) is shown in equation (19).

$$p(x,t) = f(x - ct) + g(x + ct) \quad (19)$$

Equation (19) represents a one-dimensional acoustic plane wave along the x direction. A rightward traveling plane wave is described by $f(x - ct)$ where f describes the wave shape while $(x - ct)$ propagates the wave at the speed c. Likewise, a leftward traveling wave is described by $g(x + ct)$. Knowing that acoustic waves are sinusoidal, equation (19) can be written as follows:

$$p(x,t) = A\cos(k(x - ct) + \phi_1) + B\cos(k(x + ct) + \phi_2) \quad (20)$$

with ϕ_1 and ϕ_2 being constants. By distributing k and recognizing that $kc = \omega$, and both ϕ_1 and ϕ_2 representing the phase, equation (20) can be re-written in the form below.

$$p(x,t) = A\cos(kx - \omega t + \phi_1) + B\cos(kx + \omega t + \phi_2) \quad (21)$$

The acoustic pressure can then be represented in a complex exponential form

$$\hat{p}(x,t) = \hat{A}e^{j(\omega t - kx)} + \hat{B}e^{j(\omega t + kx)} \quad (22)$$

where

$$p(x,t) = \mathrm{Re}[\hat{p}(x,t)] \quad (23)$$

with $\left|\hat{A}\right|$ and $\left|\hat{B}\right|$ representing the pressure amplitude of the rightward and leftward traveling plane waves. The phase angles of the rightward and leftward traveling waves are represented by $\arg\left[\hat{A}\right]$ and $\arg\left[\hat{B}\right]$. Similar, more detailed derivations for acoustic pressure can be found in Beranek and Kinsler [9, 10]. This analysis assumes that the pressure waves are traveling as plane waves. A wave traveling in the "X" direction will have the same pressure magnitude and phase angle at any point along the "Y-Z" plane for a given "X" position. This assumption is valid if the wavelength is much greater than the diameter of the pipe it is traveling in.

Acoustic velocity is described by the equation

$$\hat{U}(x,t) = \frac{\hat{A}}{Z} e^{j(\omega t - kx)} - \frac{\hat{B}}{Z} e^{j(\omega t + kx)} \qquad (24)$$

where Z is the characteristic impedance given by equation (25).

$$Z = \frac{\rho_o \cdot c}{s} \qquad (25)$$

and s = cross sectional area.

Knowing that the acoustic impedance of a standing wave is defined as

$$\hat{Z}(x,t) = \frac{\hat{p}(x,t)}{\hat{U}(x,t)} \qquad (26)$$

Equation (22) is divided by equation (24) and evaluated at x=0 and x=L (see Figure 2).



Figure 2. Example pipe section for equation (27)

The resultant equation is:

$$\hat{Z}_0 = \frac{\hat{Z}_L + j \cdot Z \cdot \tan(kL)}{1 + j \cdot \frac{\hat{Z}_L}{Z} \cdot \tan(kL)} \qquad (27)$$

where $\hat{Z}_0$ and $\hat{Z}_L$ are the acoustic impedances at $x = 0$ and $x = L$ respectively (see Figure 2). Equation (27) will determine the acoustic impedance of any section of pipe that is open at both ends. To determine the acoustic impedance of a pipe that is closed at $x = L$, recognize that $\hat{Z}_L$ will go to infinity.



Figure 3. Example pipe section for equation (27)

Applying the limit as $\left|\hat{Z}_L\right| \to \infty$, it can be found that

$$\hat{Z}_e = \frac{Z}{j \tan(kL)} \qquad (28)$$

$\hat{Z}_e$ is the acoustic impedance at the opening of a pipe closed on the opposite end (see Figure 3.)

The acoustic impedance at the intersection of two or more pipes can be found via the equation

$$\hat{Z}_3 = \frac{1}{\frac{1}{\hat{Z}_1} + \frac{1}{\hat{Z}_2}} \qquad (29)$$

as shown in Figure 4.

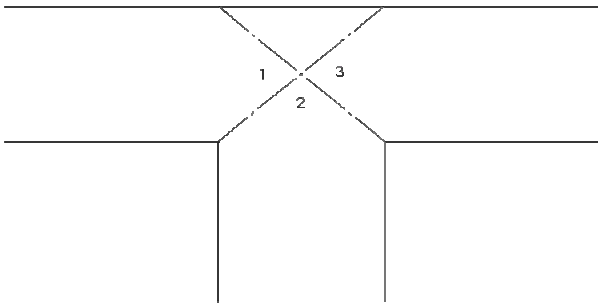


Figure 4. Example pipe section for equation (29)

By using these equations, the entire intake system can be modeled and the impedance inspected at each point in the system. Of particular interest is the impedance where there is a change in geometry within a system. Because the acoustic impedance ($\hat{Z}$) is a function of the wave number (k), which is a function of frequency, or engine speed, the log of the magnitude of the acoustic impedance is plotted against the engine speed, causing the resonant and anti-resonant frequencies to become apparent.

ACOUSTICAL TESTING

Three preliminary experiments were completed to test the validity of the impedance transfer formula as a way to measure resonant frequencies in an intake system. Three different Helmholtz resonators were studied. The geometry of each of these volumes is given in Table 1. Resonant frequencies calculated by equation (30) as well as the Impedance Transform Model are compared with experimental results in Table 2.

$$f = \frac{c}{2\pi}\sqrt{\frac{A_t}{L_t \cdot V}} \qquad (30)$$

where

f = frequency
c = speed of sound
A_t = cross sectional area of the throat
L_t = length of the throat
V = volume of the chamber.

An example of a Helmholtz resonator as tested is shown in Figure 5.

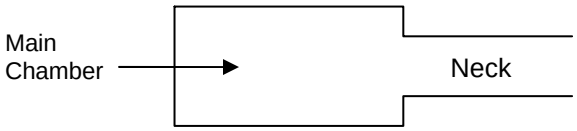


Figure 5. Example of volumes 1, 2, and 3 used in acoustic lab testing

The resonate frequency of the volumes were then calculated via the Helmholtz resonator equation and the impedance transfer formula. Experiments were then run to determine the actual resonant frequencies of the volumes. To determine the actual resonant frequencies, a microphone was placed near a loudspeaker as shown in Figure 6. A signal generator was fed through an amplifier to produce frequencies ranging from 30 – 160 Hz. The RMS voltage produced by the condenser microphone was recorded via an oscilloscope in 5 Hz intervals.

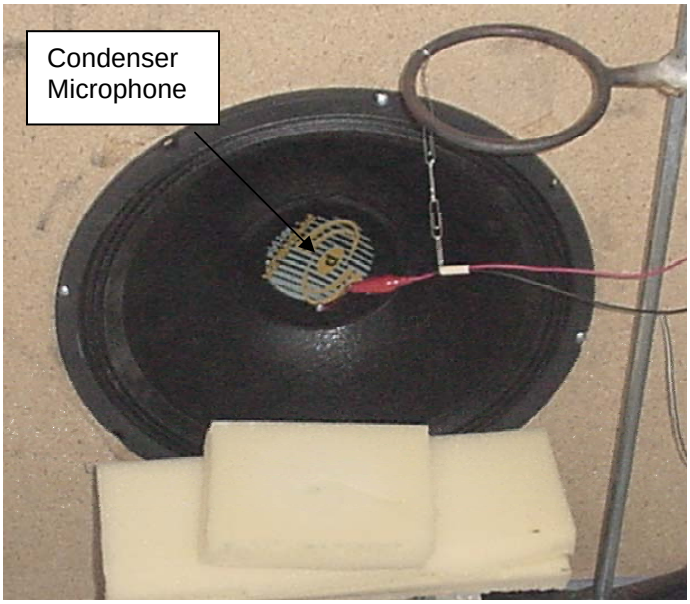


Figure 6. Condenser microphone and loudspeaker setup for baseline measurements

Each test volume was then placed with the condenser microphone at the entrance to the volume while ensuring the microphone remained in place relative to the loudspeaker. Each test volume was placed and RMS voltage measured and recorded using the same procedure as outlined above. Figure 7 shows a test volume in place for testing.



Figure 7. Measuring RMS voltage on a test volume.

By graphing the ratio of RMS voltages and noting the point at which that ratio is a local maximum, a resonant frequency could be determined. An example is shown in Figure 8 below.

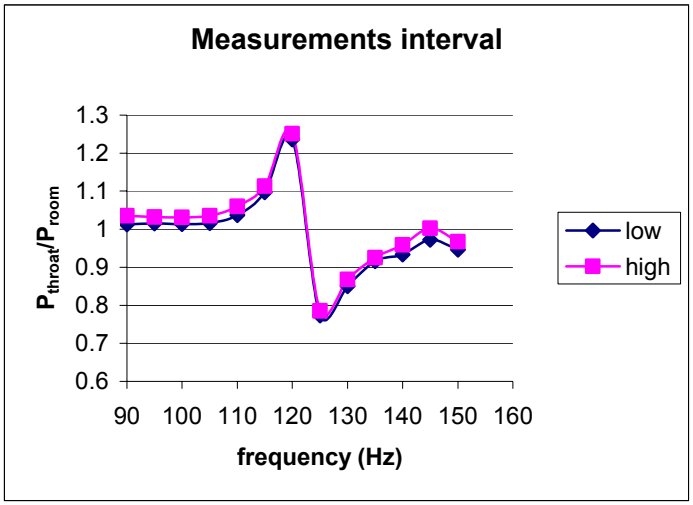


Figure 8. Graph of sound pressure ratios showing a resonant frequency at 120 Hz and an anti-resonance at 125 Hz.

Table 1. Volume dimensions as measured

	Body Length (in.)	Body Area (in2)	Neck Length (in.)	Neck Area (in2)
Volume 1	7.0	7.1	3.3	0.4
Volume 2	24.0	11.0	13.0	3.1
Volume 3	13.0	11.0	3.8	3.1

Table 2. Results of Helmholtz volume experiments

	Helmholtz frequency (Hz)	Impedance transfer frequency (Hz)	Measured resonance frequency range (Hz)
Volume #1	112	109.5	120
Volume #2	60	59	52.16 - 55.17
Volume #3	137	140	120.7 - 122.6

The results of these experiments show that the impedance transfer formula is quite robust in terms of predicting the resonance frequency of a chamber of varying shape. Further experimentation needs to be conducted to verify the impedance transfer formula's validity across an entire intake system.

ENGINE TESTING

Three different tests were performed on the engine dynamometer to verify the impedance transfer equations on an operating intake system. The intake used was a side mount plenum and runner intake with dimensions shown in Table 3. The solid model shown in Figure 9 illustrates the configuration of the inlet pipe, plenum, intake runner, and cylinder. In applying the Impedance Transform Model it was assumed that the piston location was halfway between top dead center and bottom dead center and the other three values were closed.

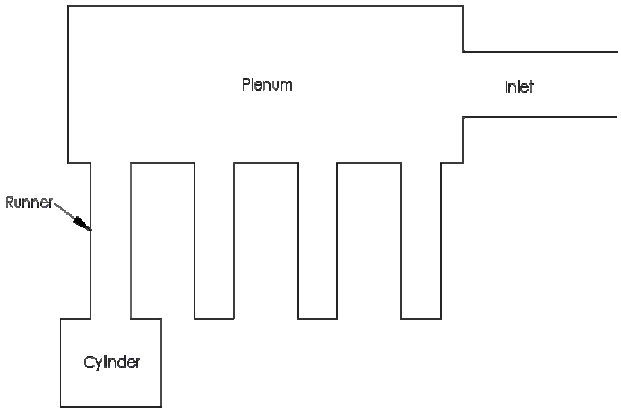


Figure 9. Sample intake components

Table 3. Critical intake system dimensions

	Length (in.)	Area (in^2)
Cylinder	1.78	5.14
Runner	8 - 11 (varied)	1.485
Plenum	11	1.85
Inlet Pipe	9.25	2.14

Figure 10 shows the impedance as a function of engine speed, taken with an 11 in. runner, for the following three locations in the intake: Zhro is the log of the absolute value of impedance at the runner/plenum junction for a runner with the intake valve open (i.e. the volume of the cylinder is taken into account), Zhrc is taken at the runner/plenum junction for a runner with the intake valve closed (assuming infinite impedance at the intake valve), and Zhinlet is taken at the start of the plenum inlet pipe.

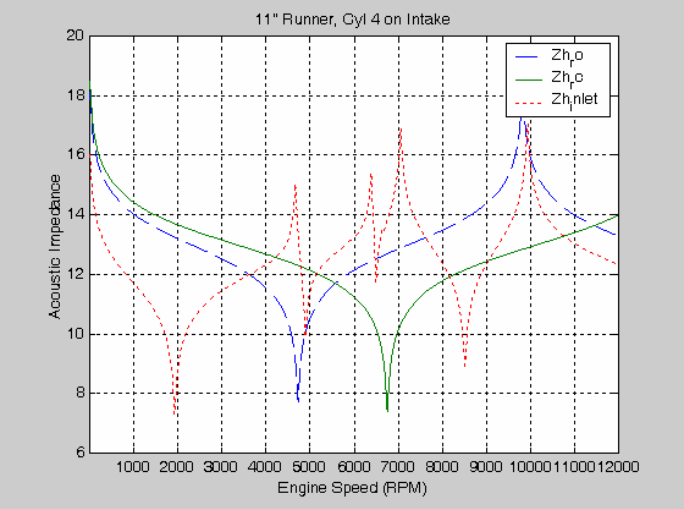


Figure 10. Impedance as a function of engine speed for 11" runner configuration.

In Figure 10, the impedance at the runner/plenum junction is plotted for both an open intake valve (Zhro) and a closed intake valve (Zhrc) to show the difference in resonance frequencies between taking into account the cylinder volume and completing an analysis based solely on the intake runners. In analyzing this plot, any activities less than 4000 RPM are ignored, as the engine cannot effectively operate at such low speeds. A peak in the torque curve can be expected at approximately 5000 RPM due to the resonance frequency of the intake runner and cylinder combination when the intake valve is open. There is also a system resonance (Zhinlet) at this engine speed with an anti-resonance immediately prior to the resonance. This would indicate a torque peak at approximately 5000 RPM with a steep slope approaching prior to the local maximum. The resonance of the intake runner with the intake valve closed (Zhrc) at approximately 6800 RPM is negated by the two sharp anti-resonances of the entire system at this same engine speed. More importantly, since the acoustics of the runner change immediately after the intake valve opens, any benefit seen from this resonance would be minimal. The entire intake system (Zhinlet) shows a strong resonance at approximately 8500 RPM with no immediate anti-resonances on either side, which indicates a broad torque increase of significant magnitude.

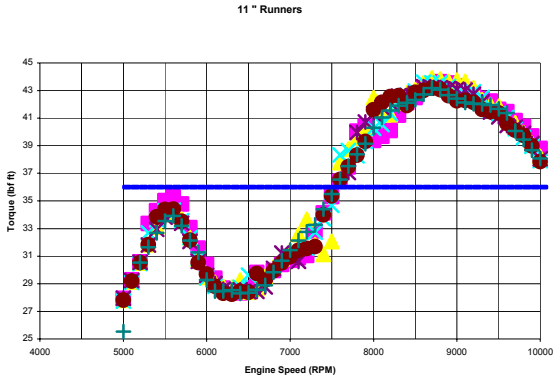


Figure 11. Torque Curve for 11" runner configuration

Figure 11 shows a torque curve with two definite resonances and one definite anti-resonance. The first definite torque peak is at 5600 RPM, which has a very steep slope on both sides of the local maximum. The next notable feature is the large dip that becomes a local minimum at approximately 6400 RPM. The torque increases again, and becomes a maximum at approximately 8700 RPM. This maximum torque corresponds with the engine speed in which the entire system is in resonance and the spacing between resonances and anti-resonances is approximately 1500 RPM, also ensuring that it is the torque peak with the largest breadth. It should be noted that this is also the region in which corresponds to the predicted maximum torque using either Engelman or Platner's methods. The increase in data scattering around 7200 and 8000 RPM is likely due to fluctuations of the dynamometer that occur during testing. The following table lists the expected peaks in volumetric efficiencies according to the three methods outlined.

Table 4. Calculation results for 8, 10, and 11 inch runners

	Engelman Model	Platner Model	Impedance Transform Model	Actual Torque Peaks
8" Runners	11500	10100	5500, 10100	5700, 10000
10" Runners	10300	8100	5000, 9000	5700, 8800
11" Runners	9800	7400	5000, 8500	5600, 8700

As shown in Table 4, Platner's method is the least accurate at predicting the torque peaks for the 11" runner, missing the final peak by approximately 1000 RPM. Engelman's method is also approximately 1000 RPM off but the engine does show a high torque at 9800 RPM. Both of the above methods only attempt to predict

the one peak, though, and do nothing to explain the other areas of the torque curve. The impedance plot accurately predicts both torque peaks and the local minimum.

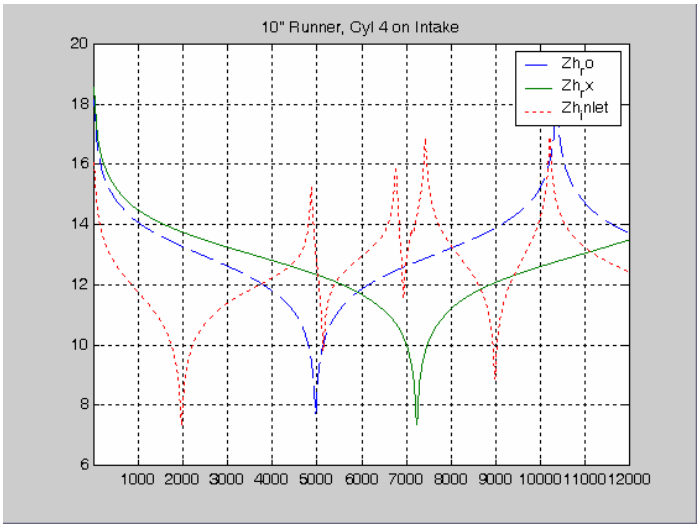


Figure 12. Impedance as a function of engine speed for 10" runner configuration.

Figure 12 shows a strong resonance from at 5000 RPM, again with both the individual runner and the intake system resonating at this engine speed, and resonances at 7200 RPM due to the runners with closed intake valves, surrounded by two immediate anti-resonances for the entire system. The anti-resonances will dominate the runner resonance for the reasons explained above and produce a dip in the torque curve as in the previous example. The entire system is shown to resonate at 9000 RPM for the intake system with ten inch runners. From the previous discussion, a small torque peak can be expected at approximately 5000 RPM with steep slopes on either side. A drop in torque would then be expected, with the minimum around 7000 RPM and finally a maximum torque occurring at approximately 9000 RPM as the entire intake system resonates.

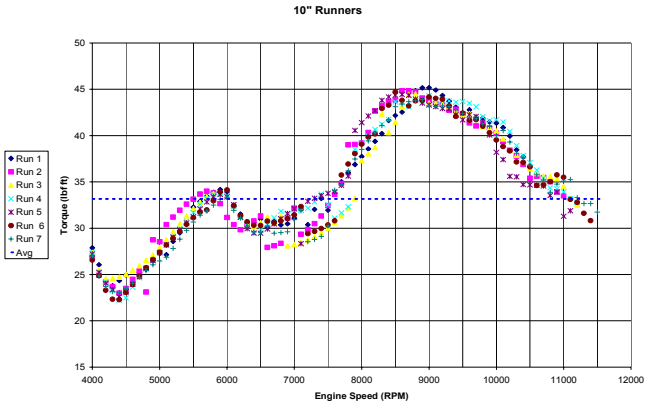


Figure 13. Torque curve for 10" runner configuration

The torque curve above shows a small torque peak at 5800 RPM and a broad torque peak at 9000 RPM. Both peaks were predicted by Figure 13 above. The predicted torque minimum occurs at 7000 RPM.

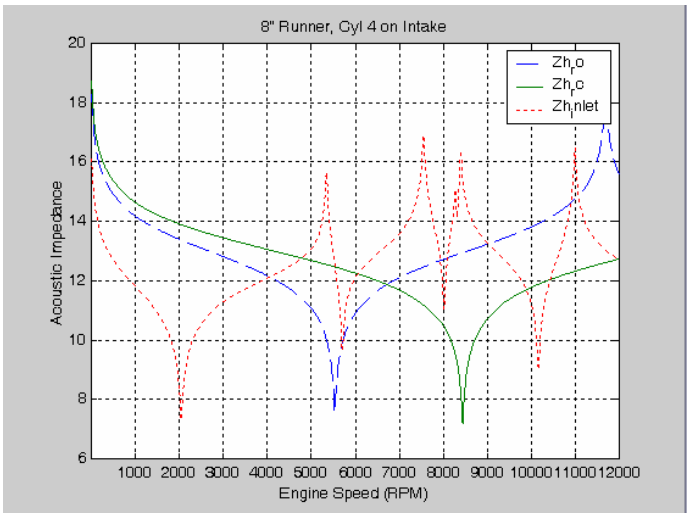


Figure 14. Impedance as a function of engine speed for 8" runner configuration.

Figure 14 shows a resonance in the runner at approximately 5500 RPM, which is expected to produce a torque peak at nearly the same engine speed. This is followed by another resonance at approximately 8000 RPM for the system and 8500 RPM for the runners with the closed intake valves. The anti-resonances in this region are spread slightly further apart than the other two examples, but one could still expect a dip in the torque curve in the 8000 RPM region. Finally, the entire system is resonating at 10,200 RPM which should produce our largest torque peak.

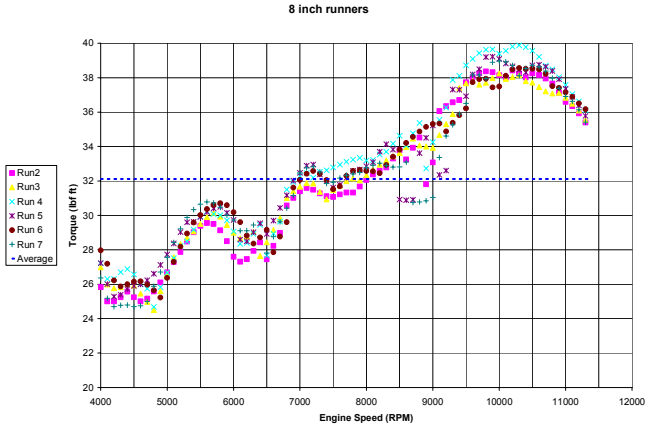


Figure 15. Torque curve for 8" runner configuration

The torque vs. engine speed in Figure 15 is relatively void of large peaks and valleys as compared to the other two examples. There is a small peak at 5700 RPM and another peak at 10000 RPM. The eleven inch runner configuration does not show the expected anti-resonance that the ten and eleven inch configurations produced. This could be due to the anti-resonances

being spread farther apart than the previous configurations.

CONCLUSION

The Platner, Engelman, and Impedance Transform Model all produce good ballpark estimates of the RPM at which an engine will reach maximum torque. Platner's formula is the simplest approach to predicting this information. The impedance transform model is the most complex method because this accounts for all aspects of intake geometry. With this model, the effect of individual intake system components can be quantified. This provides excellent feedback to the engine designer about which geometrical features are most critical in producing resonant effects.

Acoustical testing of the Helmholtz resonators provides sufficient data to show the accuracy of the model against volumes which are simple to model with the Helmholtz resonator equation. Table 2 shows the Impedance Transform Model predicting results within 3 Hz of the Helmholtz resonator equation and 20 Hz of the test results.

Dynamometer testing results shown in Table 4 show the results of the Impedance Transform Model matching within approximately 10% of the dynamometer results. The Impedance Transform Model, combined with the acoustical and dynamometer testing, is a very powerful tool for discovering the sensitivities of each intake system parameter on volumetric efficiency or torque.

The graphs shown in Figures 10, 12, and 14 show regions of resonance and anti-resonance within the intake system. Unlike the other methods discussed here, the Impedance Transform Model will not result in a numerical answer to predict torque peaks. The engine designer must be familiar with the graphs in order to accurately interpret the results and predict torque peaks. The Impedance Transform Model is intended as a tool to be used by an engine designer to help predict the multiple torque peaks and minimums as well as the slope of the torque curve. A fundamental knowledge of acoustics is required to utilize this tool.

In addition to intake systems, the Impedance Transform Model can be used to analyze exhaust systems to maximize the acoustical benefits of unsteady flow in both systems using the same technique. By slightly altering the inputs and outputs, this technique is also a valuable tool for predicting the changes in sound pressure level across a device such as a muffler or an entire intake and exhaust system to reduce the sound levels of engines.

REFERENCES

1. Ricardo, H. R. U.S. Pat. 1,834,473; 1931. "Internal Combustion Engine."
2. Platner, J. B., Moore, C. D. U.S. Pat. 2,766,743; 1956. "High Output Engine."
3. Engelman, H. W. Ph. D. Thesis, 1953, University of Wisconsin. "Surge Phenomena in Engine Scavenging."
4. Eberhard, W. W. M.S. Thesis, 1971. "A Mathematical Model of Ram-Charging Intake Manifolds for Four-Stroke Diesel."
5. Thompson, M. P. and Engelman, H. W., "The Two Types of Resonance in Intake Tuning," A.S.M.E. Paper 69-DGP-11, 1969.
6. Heywood, J. B., Internal Combustion Engine Fundamentals, McGraw-Hill, Inc., New York, 1988.
7. Blair, G. P., Design and Simulation of Four-Stroke Engines, Society of Automotive Engineers, Warrendale, PA, 1999.
8. Winterbone, D. E., and Pearson, R. J., Design Techniques for Engine Manifolds, Society of Automotive Engineers, Warrendale, PA, 1999.
9. Beranek, L. L., Acoustics, Acoustical Society of America, Woodbury, NY, 1996.
10. Kinsler, L. E., et al. Fundamentals of Acoustics, Fourth Edition, John Wiley and Sons, Inc., 2000.

CONTACT

Sammy Lee Zimmerman, MSME
University of Idaho
PO Box 440902
Moscow, ID 83844-0902
zimm2280@uidaho.edu